Zhao *et al.*
Chinese Journal of Mechanical Engineering (2023) 36:109
https://doi.org/10.1186/s10033-023-00936-z

Chinese Journal of Mechanical Engineering

ORIGINAL ARTICLE

Open Access

Grinding Characteristics of MoS_2-Coated Brazed CBN Grinding Wheels in Dry Grinding of Titanium Alloy

Junshuai Zhao[1], Biao Zhao[1], Wenfeng Ding[1*], Bangfu Wu[1], Ming Han[1], Jiuhua Xu[1] and Guoliang Liu[2]

Abstract

As an important green manufacturing process, dry grinding has problems such as high grinding temperature and insufficient cooling capacity. Aiming at the problems of sticking and burns in dry grinding of titanium alloys, grinding performance evaluation of molybdenum disulfide (MoS_2) solid lubricant coated brazed cubic boron carbide (CBN) grinding wheel (MoS_2-coated CBN wheel) in dry grinding titanium alloys was carried out. The lubrication mechanism of MoS_2 in the grinding process is analyzed, and the MoS_2-coated CBN wheel is prepared. The results show that the MoS_2 solid lubricant can form a lubricating film on the ground surface and reduce the friction coefficient and grinding force. Within the experimental parameters, normal grinding force decreased by 42.5%, and tangential grinding force decreased by 28.1%. MoS_2 lubricant can effectively improve the heat dissipation effect of titanium alloy grinding arc area. Compared with common CBN grinding wheel, MoS_2-coated CBN wheel has lower grinding temperature. When the grinding depth reaches 20 μm, the grinding temperature decreased by 30.5%. The wear of CBN grains of grinding wheel were analyzed by mathematical statistical method. MoS_2 lubricating coating can essentially decrease the wear of grains, reduce the adhesion of titanium alloy chip, prolong the service life of grinding wheel, and help to enhance the surface quality of workpiece. This research provides high-quality and efficient technical support for titanium alloy grinding.

Keywords Titanium alloy, Dry grinding, MoS_2-coated CBN wheel, Grinding wheel wear

1 Introduction

Titanium alloy has significant applications in the aerospace field due to its superior physical and mechanical properties [1–3], such as high strength, corrosion resistance, and high temperature resistance. Grinding technology, as the main method of precision processing, has been widely utilized in the processing of titanium alloy aeronautical parts [4–7]. However, due to the special chemical, physical and mechanical properties of titanium alloy, it is easy to appear adhesion and debris defects in grinding, which lead to more grinding heat and serious tool wear. Moreover, titanium alloy has the chemical reactions with cutting fluids and produces the harmful chemicals, which not only posed a threat to the health and environment of operators, but also consumed a large amount of costs in the treatment of cutting fluids, which can no longer meet the green and sustainable development consciousness [8, 9].

To solve grinding burn and meet the needs of green processing, scholars have proposed many green processing technologies such as dry cutting, cryogenic machining and minimum quantity lubrication [10–12]. From the perspective of the environment, compared with cryogenic machining and minimum quantity lubrication,

*Correspondence:
Wenfeng Ding
dingwf2000@vip.163.com
[1] National Key Laboratory of Science and Technology on Helicopter Transmission, Nanjing University of Aeronautics and Astronautics, Nanjing 210016, China
[2] AECC Zhongchuan Transmission Machinery Co., Ltd, Changsha 410200, China

dry grinding has the advantages of reducing energy consumption (such as no pumping and special equipment), and reducing resource waste (filtration device and waste liquid treatment). However, dry grinding is difficult to obtain the better machining quality. Therefore, it is important to improve the grinding condition during dry grinding, reduce the grinding temperature and ensure the grinding quality. The solid lubricant with layered structure was introduced into the grinding contact zone to form a lubricating film on the contact interface, which can minimize the friction at the grinding contact interface and reduce the thermal damage strength to a certain extent [13].

Matthew et al. [14] applied the different solid lubricants in grinding and found that the non-toxic solid lubricants can reduce costs, protect the environment, and improve the quality of ground surface. Adhakrishnan et al. [15] studied the comparative test of dry grinding with graphite as lubricant and traditional grinding, and confirmed that graphite assisted dry grinding has better grinding quality, and the grinding force and temperature have been greatly improved. Shaji et al. [16] research shows that when there are sufficient lubrication conditions in the grinding area, the friction coefficient of the ground surface will be reduced. At the same time, the burn of the ground surface can be avoided and the grinding quality can be improved. Rahmati et al. [17] developed a nano-lubricant containing MoS_2 nanoparticles for the milling of AL6061-T6 alloy. The rolling action of the nanoparticles at the tool-workpiece interface significantly reduced the cutting forces and effectively improved the surface morphology of the machined workpiece. Ding et al. [18] designed a self-lubricating grinding wheel. The solid powder lubricant is blown out of the grinding wheel cavity to the grinding surface by centrifugal force, thus improving the friction and wear performance of the grinding wheel during grinding. Mahathanabodee et al. [19] added hexagonal boron nitride solid lubricant to 316L stainless steel composites and found that the addition of lubricant can effectively improve the friction properties of materials. Zhao et al. [13] prepared MoS_2 embedded metal composites by liquid phase sintering. The friction properties of different samples of solid lubricants with different concentrations were evaluated. The results showed that MoS_2 samples had better mechanical and tribological properties at the same lubricant concentration.

The above research shows that the grinding quality and friction and wear properties of materials can be effectively improved by introducing solid lubricants. However, there is little research on the influence of solid lubricants on the dry grinding of titanium alloys, and the above research requires the preparation of special lubricant feeding devices or the preparation of mixed abrasive wheels through special processes. The combination of solid lubricant and cubic boron nitride (CBN) orderly arranged grinding wheel by means of coating can not only make use of the advantages of ordered arrangement of CBN grinding wheel and solid lubricant to realize the research of titanium alloy dry grinding process, but also the realization method is simple and easy to operate. Therefore, in this study, MoS_2 is used as the solid lubricant coating material of CBN orderly arrangement grinding wheel (MoS_2-coated CBN wheel), and the dry grinding tests with MoS_2-coated CBN wheel in titanium alloy materials were carried out. The lubrication mechanism of MoS_2 solid lubricant in the grinding process is analyzed. The influence of grinding parameters on grinding force, grinding temperature and surface roughness, as well as the characteristics of grain wear in the grinding process are analyzed, which provides technical support for efficient and high-quality grinding of titanium alloy.

2 Materials and Methods

2.1 Lubrication Mechanism of Solid Lubricating Coating

The lubrication mechanism of solid lubricant is that the solid lubrication phase is coated on the surface of abrasive grains by organic bonding hot coating method, forming a lubrication film between workpiece and abrasive grains. The lubrication layer can improve the grinding environment in the contact zone, inhibit abrasive particle adhesion wear, reduce the temperature, and achieve the purpose of improving the grinding performance of titanium alloy [20]. The abrasive grains slip on the surface of the titanium alloy. With the action of load, grains are pressed into the titanium alloy. If the contact area increases, the friction will also increase, and the furrow phenomenon will occur, as shown in Figure 1(a). If the abrasive grains slip directly

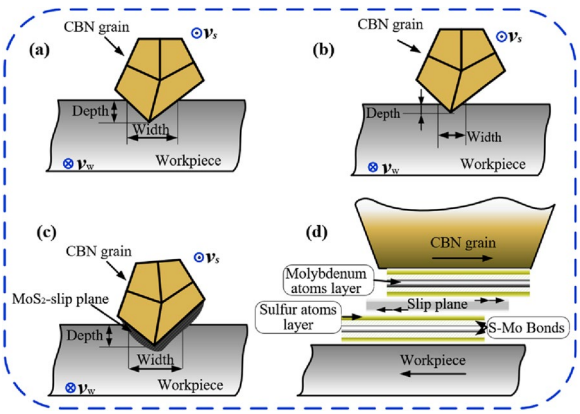

Figure 1 Friction and wear model of abrasive grains in solid lubricating coating: (**a**) Cut into workpiece, (**b**) Slip on workpiece surface, (**c**) Solid lubricated grain cut into workpiece and (**d**) solid lubrication mechanism

on the surface of titanium alloy, although the contact area will not increase, due to the temperature rise of the friction surface, occlusion is easy to occur, as shown in Figure 1(b). As shown in Figure 1(c), there is a solid lubricant between the two friction surfaces, and its shear resistance is very small, so the external friction between the two friction surfaces is transformed into the internal friction between the molecules of the solid lubricant. As shown in Figure 1(d), the solid lubrication mechanism of solid lubrication film is a solid lubricant with layered structure, which has sliding characteristics under the action of shear force.

The abrasive grains and the workpiece are separated by solid lubrication coating at the beginning of cutting, and the friction (F_f) generated is only the shearing force (F_τ) generated inside the solid lubricant. At this time, the F_f can be expressed as follows:

$$F_f = F_\tau = A_r \tau_c, \tag{1}$$

where A_r is the actual contact area, which can be obtained from the following formula [21]:

$$A_r = \pi \left[\sqrt[3]{\frac{3PR}{4E}} \right]^2, \tag{2}$$

where R, E and P are the radius of curvature of the contact arc region, the elastic modulus of the substrate and the load, respectively. At this time, the friction coefficient μ can be expressed as:

$$\mu = F_f / P = \pi \frac{\tau_c}{\sqrt[3]{P}} \left[\sqrt[3]{\frac{3R}{4E}} \right]^2. \tag{3}$$

As the grinding progresses, a lubricating film is formed under the action of pressure and friction, which is in a state of boundary lubrication. The ultimate shear stress of the solid lubricating film is τ_{cmax}, and it is assumed that $\tau_{cmax} = d\tau_0$, τ_0 is the shear strength limit of the MoS_2 solid lubricating film. The premise for the isolation and friction reduction of the MoS_2 solid lubricating film between the grinding wheel and the material surface is as follows [22]:

$$\sigma^2 + k\tau_{c\max}^2 = \sigma_0^2, \tag{4}$$

where k is a constant of $k > 1$, σ_0 is the compression yield limit of titanium parts, and σ is the normal compressive stress formed by the normal load. According to the basic theory of adhesive friction, $k{\tau_0}^2 = {\sigma_0}^2$, the friction coefficient μ can be expressed as follows:

$$\mu = \frac{\tau_{c\max}}{\sigma} = \frac{d}{[k(1-d^2)]^{1/2}}. \tag{5}$$

It can be concluded that the friction force at this time is a constant value. The lubricant has been coated on the surface of the abrasive, and there is no need for a penetration process. The solid lubricating coating can withstand a lot of pressure. With the reduction of the relative sliding speed of the friction surface of the moving pair and the reduction of the lubricant thickness and surface roughness, the friction surface is too close, so the micro convex contact increases, thus entering the boundary lubrication state. At this time, the tribological properties between the friction surfaces will be determined by the interaction between the lubricant and the surface and the properties of the generated boundary film. Therefore, when there is a layer of MoS_2 lubricating film between the abrasive grains and titanium alloys surface, the friction coefficient μ is reduced.

2.2 Test Device and Method

The specific steps for the preparation of MoS_2-coated CBN wheel used in this study are as follows: Firstly, MoS_2 lubricant powder is passed through a sieve, the lubricant phase powder is selected and baked in oven for two hours. Secondly, the selected binder polyvinyl butyral and the lubricating phase powder are mixed in a certain proportion in a sealed vessel, and placed in an ultrasonic cleaner for ultrasonic vibration for one hour. And then evenly coat it to wheel abrasive grains, then dry it in the natural environment for 24 h. The prepared MoS_2-coated CBN wheel is shown in Figure 2.

The material properties of Ti-6Al-4V are shown in Table 1, and the sample size of the workpiece is 60×10×50 mm, ground surface size: 50×10 mm. The test was carried out on the DMG machining center (ULTRASONIC 20 linear, spindle speed range: 40000 r/min), and the test device is shown in Figure 3. Before

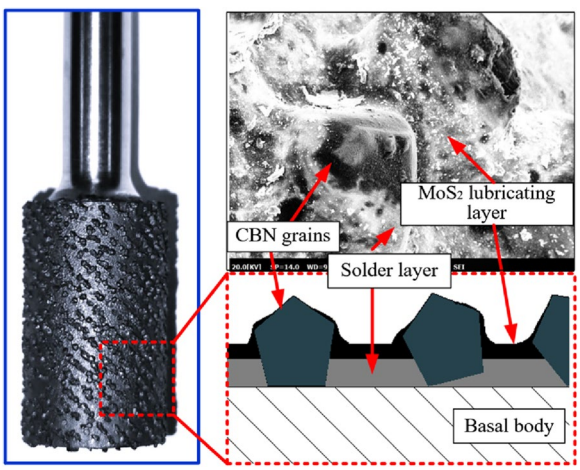

Figure 2 Single layer brazed CBN grinding wheel with MoS_2 coated

Table 1 Ti-6Al-4V material properties

Workpiece material	Density ρ(g/cm^3)	Elastic modulus E(GPa)	Yield strength σ(MPa)	Poisson's ratio v
Ti-6Al-4V	4.62	117.6	930	0.36

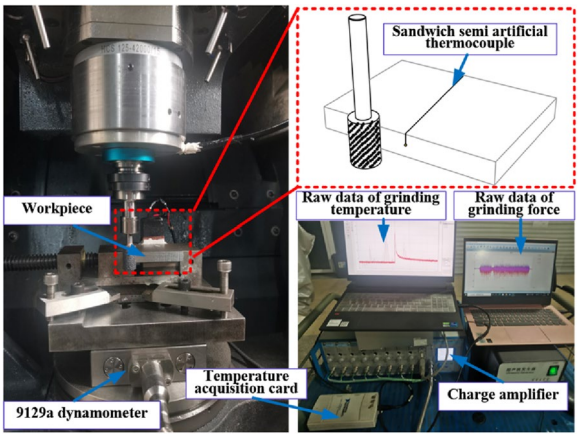

Figure 3 Grinding test device

Table 2 Experimental parameters

Contents	Values
Grinding model	Up-grinding
Type of grinding wheel	Brazed CBN grinding wheel (40 /50 #)
Specification	12 mm×20 mm
Arrangement mode	Single layer orderly arrangement (space: 1.2 mm)
Grinding width b	10 mm
grinding speed v_s	5–20 m/s
Feed speed v_w	800–2400 mm/min
Grinding depth a_p	5–20 μm

the grinding test, all grinding wheels need to be reshaped and sharpened, so that the grinding wheels are in the same state before grinding. In this paper, a single-layer brazed CBN wheel (common CBN wheel) and MoS_2-coated CBN wheel are used to carry out dry grinding tests on titanium alloy materials. The CBN grains on the wheel are arranged in an orderly manner. Table 2 shows the wheel parameters and grinding parameters. And the grinding temperature and grinding force during grinding were measured by artificial thermocouple and 9129A dynamometer. Use the roughness meter to detect the roughness value on the machine, measure three different positions, and calculate the average value as the final result of each group of tests. Three-dimensional video and SEM were used to extract the surface morphology, abrasive grain height and distribution characteristics of the grinding wheel after each group of tests, and analyze the grinding wheel wear degree.

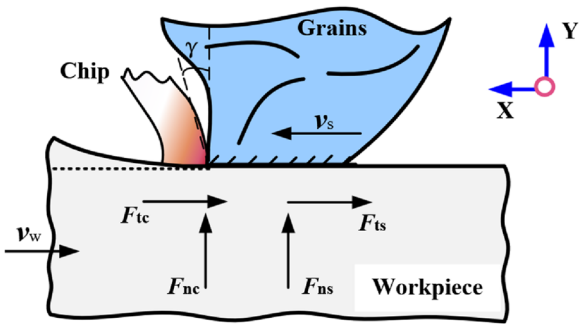

Figure 4 Composition of grinding force

3 Results and Discussion

3.1 Grinding Force

The grinding process can be divided into three stages of rubbing, ploughing and cutting [23]. Through the extrusion of the abrasive grains on the metal material, the metal layer produces elastic-plastic deformation and shear slip. When the strain of the material in the grinding area reaches a certain value, the material peels off the workpiece in the form of debris. As shown in Figure 4, the grinding force can be decomposed into the cutting force on the abrasive rake face and the sliding friction force on the blunt face in the contact area. If the contact mode of the abrasive contact area is regarded as the form of sliding friction, the grinding force is decomposed according to the tangential and normal directions [24]:

$$F_t = F_{tc} + F_{ts} = (F_x \cos\gamma + F_y \sin\gamma) + F_y', \tag{6}$$

$$F_n = F_{nc} + F_{ns} = (F_x \sin\gamma - F_y \cos\gamma) + F_x', \tag{7}$$

where F_t, F_{tc} and F_{ts} are tangential grinding force, tangential grinding force generated in cutting action and sliding friction tangential grinding force respectively. F_n, F_{nc} and F_{ns} are normal grinding force, normal grinding force generated in cutting action and normal grinding force caused by sliding action respectively. γ, F_x, F_y, F_x' and F_y' are the absolute values of the rake angle of the abrasive grains, the positive pressure in the normal direction of the grain contact surface, the sliding friction in the tangent direction of the grain contact surface, the positive pressure on the wear plane and the sliding friction along the tangent direction of the wear plane, respectively. Therefore, the relationship between F_t, F_n and sliding friction coefficient μ is as follows:

$$F_t = F_{tc} + F_{ts} = (F_x \cos\gamma + \mu F_x \sin\gamma) + \mu F_x', \quad (8)$$

$$F_n = F_{nc} + F_{ns} = (F_x \sin\gamma - \mu F_x \cos\gamma) + F_x'. \quad (9)$$

Assuming that the pressure per unit area among the grain and the contact material is F_p, the contact area among the grain and the contact material is S_c, the pressure per unit area at the abrasive wear plane is F_p', and the surface of impact among the grain and the machined surface is S_{ls}, the following relationship can be obtained:

$$F_t = F_p S_c(\cos\gamma + \mu\sin\gamma) + \mu F_p' S_{ls}, \quad (10)$$

$$F_n = F_p S_c(\sin\gamma - \mu\cos\gamma) + F_p' S_{ls}. \quad (11)$$

It can be seen from the analysis in Section 2.1 that the sliding friction coefficient of the MoS_2-coated CBN wheel is smaller than that of the common CBN wheel. Because of the existence of the lubricating layer, the contact area S_c between the grains and the contact surface decreases. Therefore, the following relationship exists:

$$F_{t(wt)} > F_{t(MoS_2)}, \quad (12)$$

$$F_{n(wt)} > F_{n(MoS_2)}. \quad (13)$$

The variation of grinding force with grinding parameters is shown in Figure 5. With the increase of cutting depth a_p, the normal force F_n and tangential force F_t of both MoS_2-coated CBN wheel and common CBN wheel increase significantly (Figure 5(a)). The reason is that when the grinding wheel speed v_s and workpiece speed v_w are constant, increasing the cutting depth a_p, the depth of grain cutting into the material increases, and the maximum undeformed thickness h_{max} increases. Moreover, the pressure F_p per unit area among abrasive grains and grinding arc area increases, the contact area S_c among grains and grinding area increases, and the F_n increases. Similarly, the F_t also shows an increasing trend. At the same time, the geometric contact arc length among the wheel and the workpiece also increases, and the dynamic effective grains involved in grinding increase, so the grinding force increases. During grinding, the feed speed v_w increases and the grinding force gradually increases (Figure 5(b)). With the increase of v_w, the contact area between grains and workpiece increases in unit time, and the cutting area of abrasive grains on materials increases, and the removal volume increases. When the grinding depth is certain, the pressure F_p per unit area among grains and grinding arc area remains unchanged, the contact area S_c among grains and grinding arc area increases, and the F_n increases. Similarly, the F_t also shows an

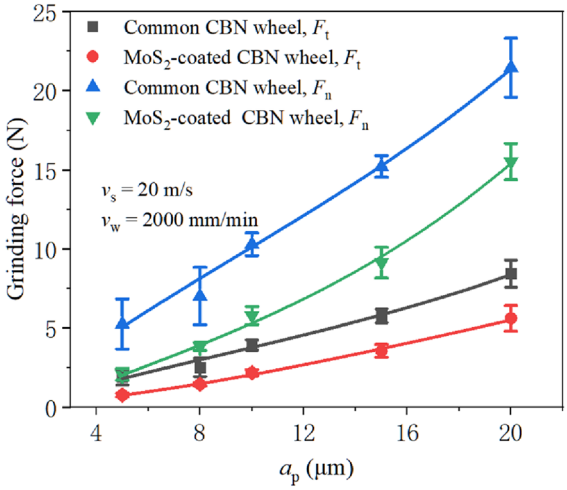

(a) Influence of a_p on grinding force

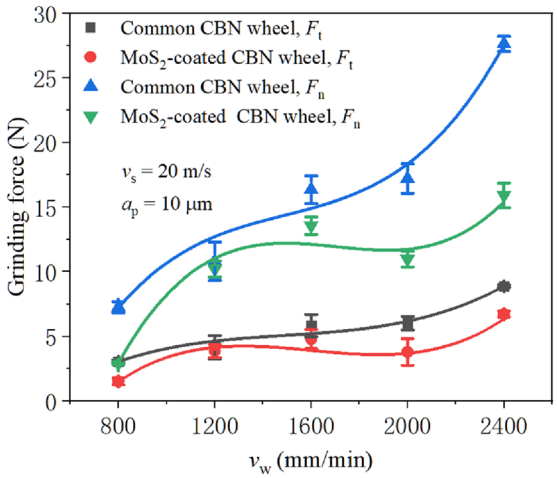

(b) Influence of v_w on grinding force

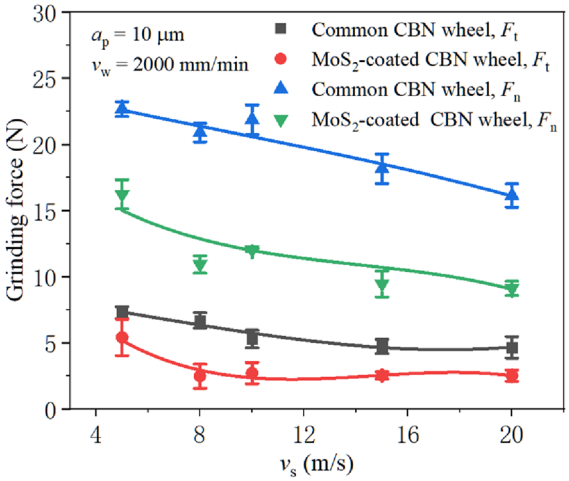

(c) Influence of v_s on grinding force

Figure 5 Influence of grinding parameters on grinding force

increasing trend. The grinding force under different wheel speeds v_s is shown in Figure 5(c). the wheel speeds v_s increases and the grinding force gradually increases. when v_s is from 5 m/s to 15 m/s, the force in grinding of these two types of grinding wheels is greatly reduced, and when v_s is from 15 m/s to 20 m/s, the force in grinding of these two types of grinding wheels is slowly decrease. With the increase of v_s, the time of a single abrasive grain in the grinding arc area decreases. And, more abrasive grains participate in grinding, reducing the wear of the abrasive blade, and intensifying the "sliding friction" effect on the workpiece material. Therefore, the force in grinding shows a slow downward trend.

From Figure 5, it is known that the force in grinding of MoS_2-coated CBN wheel is lower than that of common CBN wheel under the same conditions. It is known from the above analysis that the sliding friction coefficient μ_{MoS2} of the MoS_2-coated CBN wheel is smaller than the sliding friction coefficient μ_{wt} of the common CBN wheel, which reduces the friction of grain cutting materials. On the other hand, due to the lubricating effect of MoS_2, the wear behavior of the abrasive grains during the grinding process is weakened, and the grinding edge is relatively sharp. When $v_s = 20$ m/s, $v_w = 2400$ m/min, $a_p = 10$ μm, the normal grinding force F_n is reduced by 42.5% at the maximum, and the tangential grinding force F_t at this time is reduced by 28.1%.

3.2 Grinding Temperature

The energy predominantly exists as grinding heat during the grinding process, and minor grinding heat will disperse with the chips, and most of them accumulates in the grinding arc area [25–27]. The grinding temperature at the contact point between the grains and the workpiece is the highest, which is also the heat source of the grinding process. Grinding temperature is an intuitive manifestation of the effect of abrasive grains on material removal in the grinding of Ti-6Al-4V materials. Therefore, this paper analyzes the influence law between grinding temperature and grinding parameters. Semi- artificial thermocouple device is used to collect the temperature generated in grinding (Figure 3), and use standard thermocouple to calibrate the corresponding relationship between potential U and temperature T in Ti-6Al-4V and constantan wire system. The calibration function is as follows [28]:

$$T = 0.0108U^3 - 0.154U^2 + 23U + 27. \quad (14)$$

Figure 6 shows the comparison of the influence trend of grinding parameters of two kinds of wheels on grinding temperature. The relationship between grinding depth a_p and grinding temperature shows the trend in Figure 6(a). In the process of increasing a_p from 5 μm to 20 μm,

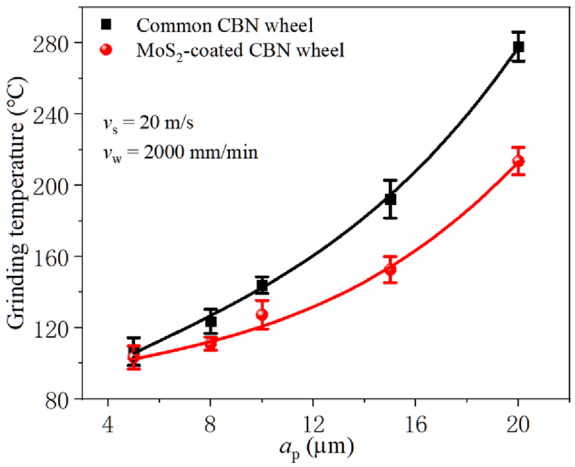

(a) Influence of a_p on grinding temperature

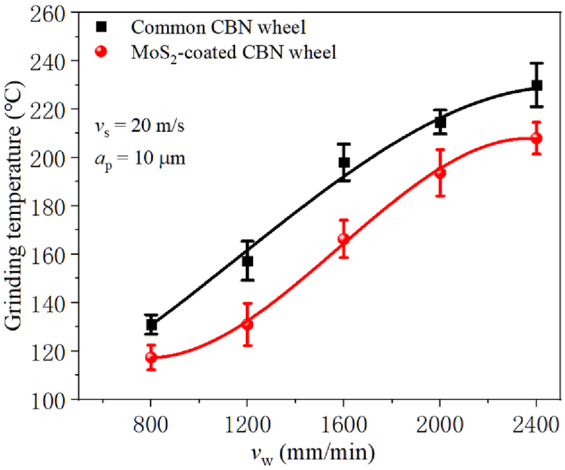

(b) Influence of v_w on grinding temperature

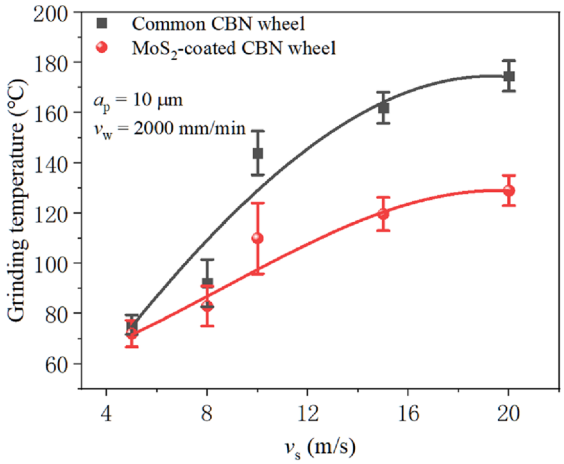

(c) Influence of v_s on grinding temperature

Figure 6 Influence of grinding parameters on grinding temperature

the grinding temperature of MoS_2-coated CBN wheel increased from 103.3 ℃ to 213.7 ℃, increased by 106.9%, and the grinding temperature of common CBN grinding wheel increased from 106.7 ℃ to 278 ℃, increased by 160.5%, showing a sharp upward trend, but no burns occurred within the test parameters. With the increase of a_p, the friction force and cutting depth of grains on the workpiece surface increase, and the material removal thickness increases, and the capacity consumed in the processing process increases, therefore, the grinding specific energy increases and the temperature increases. The grinding temperature increases gradually with the increase of the feed rate v_w, as shown in Figure 6(b). The increase of v_w will speed up the movement of the grinding heat source, but the contact area among the grains and the workpiece material adds in per unit time, then the cutting area of grains on the material rises, and cutting thickness and grinding temperature rises. Under the comprehensive effect that the heat generation effect is greater than the heat dissipation effect, the grinding temperature shows an upward trend. The relationship between grinding speed v_s and grinding temperature shows the trend in Figure 6(c). With the increase of v_s, the time for grains to act on the grinding arc area decreases. In a certain period of time, more abrasive grains participate in grinding, resulting in the intensification of the "sliding friction" effect of abrasive grains on the workpiece material. Therefore, more energy is converted into grinding heat in the grinding arc area.

According to the analysis of grinding temperature, the grinding temperature is at a low level within the range of parameter selection (Figure 6). Brazed CBN grinding wheel abrasive grains are arranged in an orderly manner to optimize the landform, high abrasive exposure, large chip holding space, and the grinding wheel is not easy to be blocked. MoS_2-coated CBN wheel adds MoS_2 lubricant on the basis of brazing CBN grinding wheel, which provides a carrier for heat flow, reduces friction heat energy and reduces grinding temperature. When $v_s = 20$ m/s, $v_w = 2000$ mm/min and $a_p = 20$ μm, the grinding temperature decreases by 30.5%. Moreover, due to the orderly arrangement of the abrasive grains of the brazed grinding wheel, the large chip holding space between the abrasive grains is full of lubricant. After the lubricant on the surface of the abrasive grains are worn, the lubricant between the abrasive grains play a complementary role and prolongs the service life of the lubricating coating.

3.3 Grinding Wheel Grain Wear

Due to the characteristics of the grinding wheel, grains wear is inevitable during the entire grinding process. Severe grinding wheel wear affects the geometric accuracy and surface quality of the workpiece [29, 30], Therefore, the study of grain wear is an important means to evaluate the performance of grinding wheel.

As the material removal volume V_w increases, the grain wear morphologies of the two grinding wheels are shown in Figure 7. When V_w reaches 400 mm^3, the cutting edges of the two types of grinding wheel grains have different degrees of wear. When V_w increased from 400 mm^3 to 800 mm^3, the grains of both grinding wheels were slightly broken, but no grains fell off, and no obvious chips adhered to the grinding wheel. At this time, the grain micro damage of common CBN wheel was relatively serious. When the V_w increased from 800 mm^3 to 1200 mm^3, the grains of the two grinding wheels were broken in large pieces, and the common CBN wheel grains have obvious titanium alloy chip adhesion. From the microstructure around the grain of the MoS_2-coated CBN wheel, it can be seen that there is good infiltration between the lubricant and CBN grains, and there is no chip adhesion.

The mathematical statistics method is used to analyze the wear of the grinding wheel grains. According to the change of grinding wheel grain wear state with the amount of material removed, the wear types (no wear, abrasion wear, micro-fracture, macro-fracture) and distribution rules of CBN grains are counted, the height difference between the exposed height of grains and the grinding wheel matrix is measured and calculated, and the grinding wheel grain wear is quantified, as shown in Figure 8. Gaussian distribution probability density function is adopted as follows [31, 32]:

$$f(h) = \frac{1}{\sqrt{2\pi}} \exp\left[-\frac{(h-\mu)^2}{2\sigma^2}\right], \tag{15}$$

where h, μ and σ represent the contour height of grain relative to matrix, the mean value of contour height and the standard deviation of contour height, respectively.

The protruding height and wear morphology of CBN grains on the surface of the grinding wheel were measured by a three-dimensional video microscope, each group randomly collects 60 grain data as the basis. The Gaussian distribution of the grain bulge height is shown in Figure 9, and the wear type distribution of CBN grains is shown in Figure 10. By analyzing the mean probability density of the initial protruding height of CBN grains, the average protruding height of MoS_2-coated CBN wheel abrasive grains is 291.53 μm, and the average protruding height of common CBN wheel abrasive grains is 351.08 μm. This is because the MoS_2-coated CBN wheel grains are arranged in an orderly manner, the large chip space between the abrasive grains is filled with lubricant, and the height difference from the highest point of grain and the matrix is reduced.

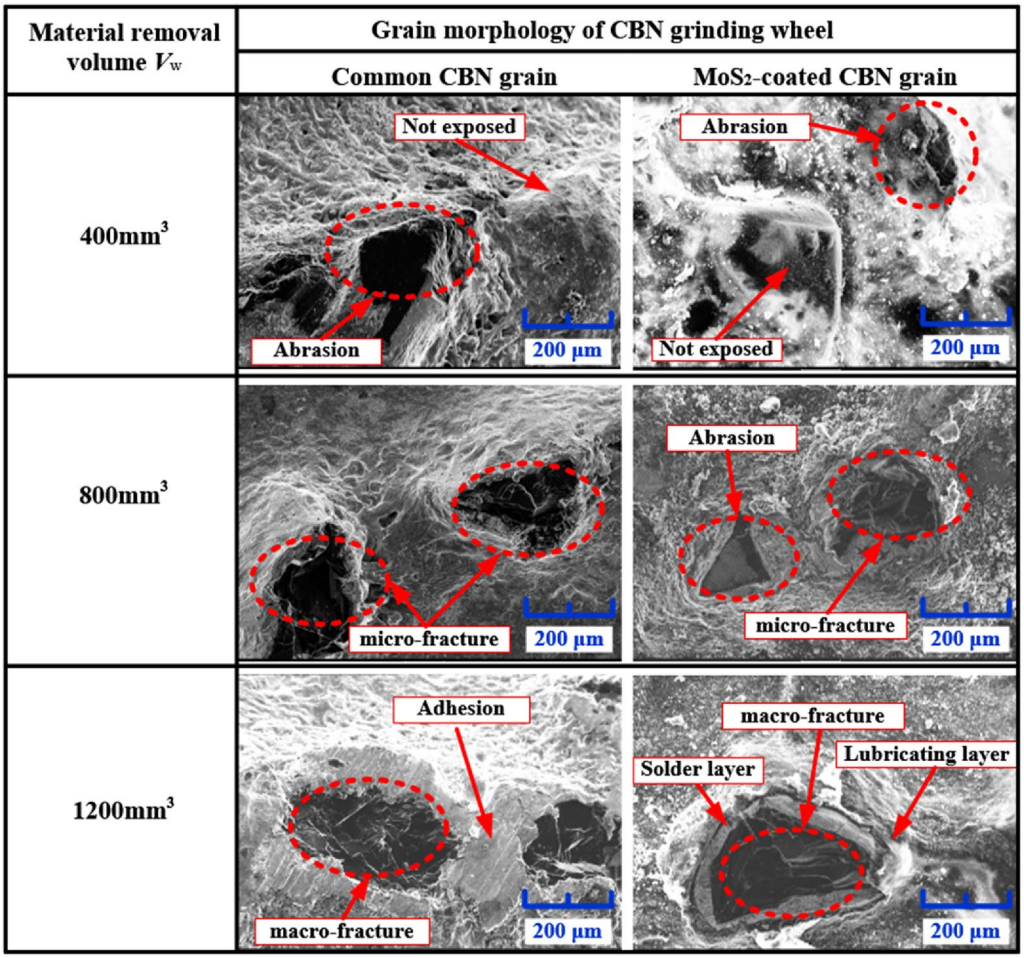

Figure 7 Evolution of abrasive wear morphology of two CBN grinding wheels (V_w=400–1200 mm^3)

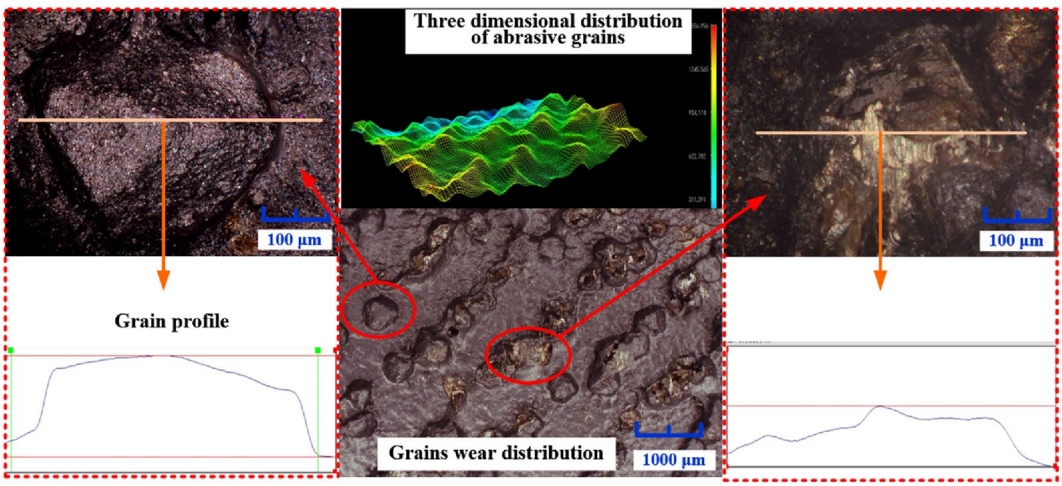

Figure 8 Grain morphology of grinding wheel under three-dimensional video microscope

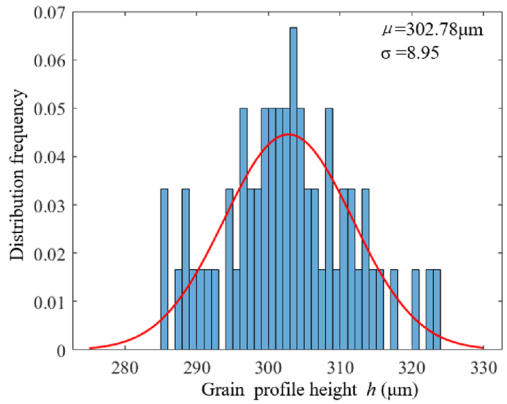

(a) Common CBN grains height distribution histogram (V_w=400 mm^3)

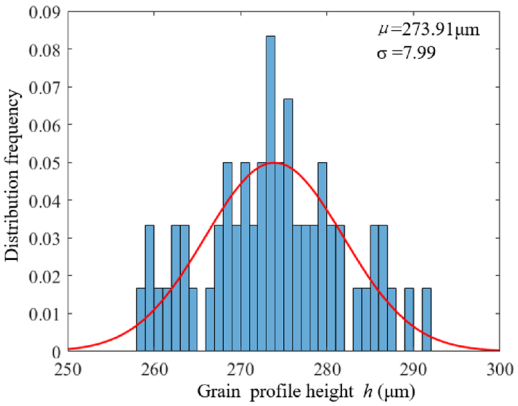

(b) MoS_2-coated CBN grains height distribution histogram (V_w=400 mm^3)

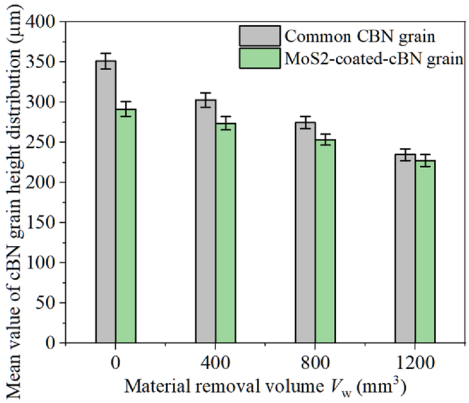

(c) Abrasive grains height distribution

Figure 9 Gaussian distribution diagram of grain bulge height and statistical diagram of average contour height

Figure 9(a, b) respectively show the height profile histograms of the grains of MoS_2-coated CBN wheel and common CBN wheel when the material removal amount reaches 400 mm^3. Due to the limited number of CBN grains collected, the standard deviation of the figure

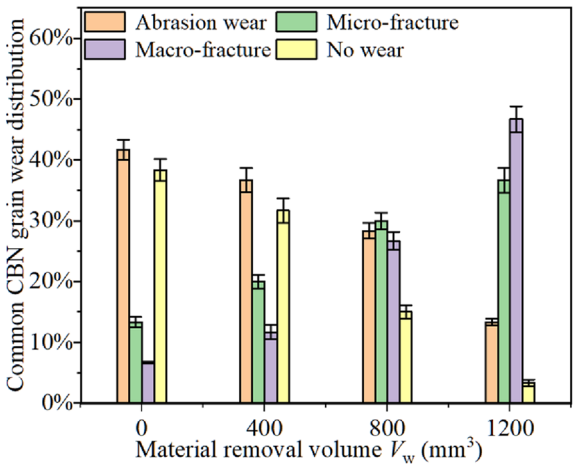

(a) Common CBN wheel grain wear

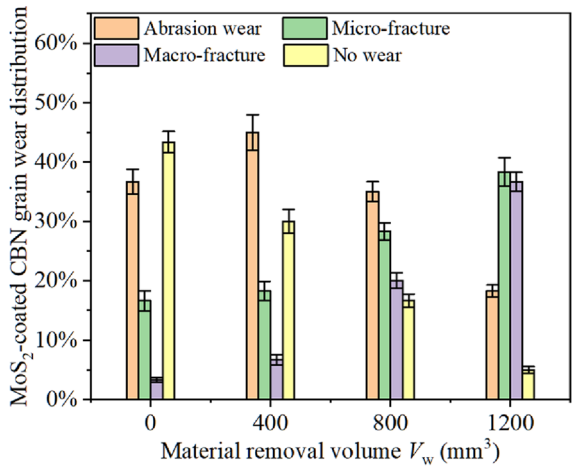

(b) MoS_2-coated CBN wheel grain wear

Figure 10 The type and proportion of CBN grain wear with the increase of material removal

obtained is large. Figure 9(c) shows the trend of the average grain height distribution with the material removal volume. When the V_w reaches 400 mm^3, the average protruding height of grains of MoS_2-coated CBN wheel is 273.91 μm, the average protruding height of grains of common CBN wheel is 302.79 μm, and the wear height of the common CBN wheel is obviously larger. When the V_w reaches 1200 mm^3, the average protruding height of MoS_2-coated CBN wheel abrasive grains is 227.39 μm, and the average protruding height of abrasive grains of common CBN wheel is 234.82 μm. It can be seen that MoS_2 lubricant can effectively slow down the wear of grinding wheel grains.

The type and distribution of grinding wheel grain wear are shown in Figure 10. Figure 10(a) shows the variation law of abrasive wear type of common CBN grinding wheel with V_w. With V_w increasing to 400 mm^3, the CBN

grains that did not participate in grinding accounted for about 31.7%, the CBN grains with micro-fracture and macro-fracture increased slowly from 13.3% and 6.7% to 20% and 11.7%, respectively, and the CBN grains with abrasion wear decreased from 41.7% to 36.7%.When V_w continued to increase to 1200 mm^3, the proportion of CBN grains that did not participate in grinding rapidly decreased to about 3.3%, while the CBN grains with micro-fracture and macro-fracture rapidly increased to 36.7% and 46.7%, and the CBN grains with abrasion wear continued to decrease to about 13.3%. The grain wear type and distribution law of MoS_2-coated CBN wheel are shown in Figure 10(b). It can be seen that as V_w increases to 400 mm^3, about 30% of CBN grains did not participate in grinding, the CBN grains with micro-fracture and macro-fracture slowly increase from 16.7% and 3.3% to 18.3% and 6.7%, respectively, and the CBN grains with abrasion wear increase from 36.7% to 45%. When V_w continued to increase to 1200 mm^3, the proportion of CBN grains that did not participate in grinding rapidly decreased to about 5%, while the CBN grains with micro-fracture and macro-fracture rapidly increased to 38.3% and 36.7%, and the CBN grains with abrasion wear continued to decrease to about 18.3%. This indicates that with the increase of material removal volume, some CBN grains with higher exposed heights take part in grinding first, and wear and tear, micro-fragmentation and even big fragmentation occur under heavy load. Most of CBN grains with lower exposed heights also take part in material removal gradually with the fragmentation of surrounding grains. Comparing the two grinding wheels, it is found that MoS_2 lubricant can effectively reduce the wear of the grinding wheels and prolong the service life of the grinding wheels.

3.4 Ground Surface Quality

Figure 11 shows the influence of grinding parameters on the surface roughness of titanium alloy ground with MoS_2-coated CBN wheel and common CBN wheel. To reduce the measurement error, three measurement points are accumulated under each group of grinding parameters to obtain the mean value. When the grinding depth a_p changes from 5 μm increased to 20 μm. The surface roughness of the workpiece increases significantly (Figure 11(a)). The increase of a_p and the increase of the depth of grain ploughing into the workpiece lead to the longer stroke of abrasive grains contacting the workpiece material. Therefore, there are deep cutting marks on the surface of the workpiece, and the roughness increases. The effect of different feed speeds v_w on the surface roughness is shown in Figure 11(b). When the feed speeds v_w changes from 800 mm/min to 2400 mm/min, the surface roughness of the workpiece first increases,

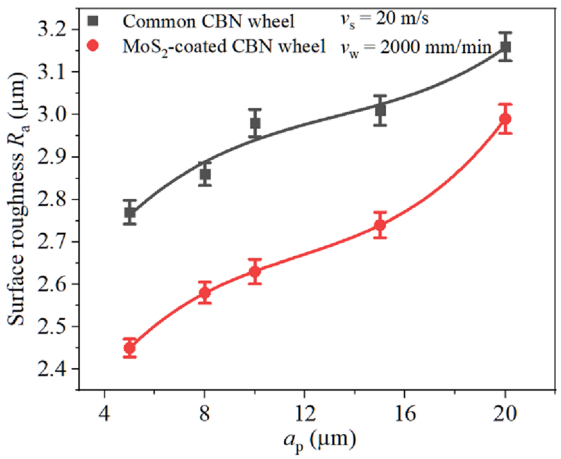

(a) Influence of a_p on ground surface roughness

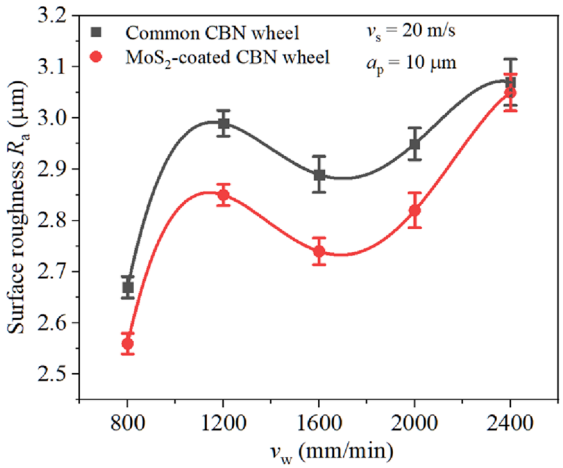

(b) Influence of v_w on ground surface roughness

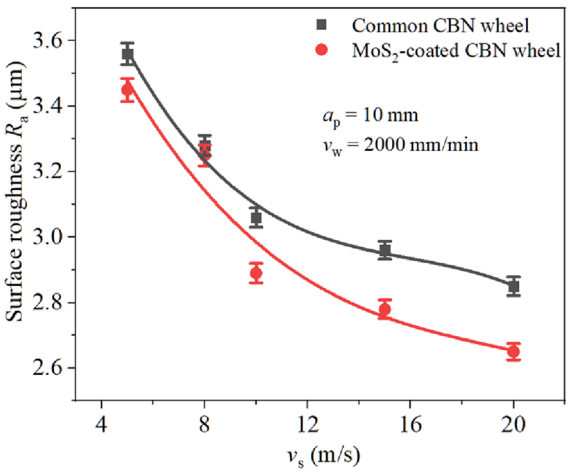

(c) Influence of v_s on ground surface roughness

Figure 11 Influence of grinding parameters on ground surface roughness

then decreases and then increases. The main reason is that due to the increase of v_w, the cutting thickness of single abrasive grains also increases, the grinding force increases and the roughness increases. Under the action of tangential force, the cutting edges of some highly exposed abrasive grains are worn and broken, forming multi-edge cutting. And the low exposure abrasive grains participate in the material removal, and the roughness is improved [33]. At this time, it is beneficial to reduce the surface roughness by selecting a lower speed of the workpiece for grinding the surface. When the grinding speed v_s changes from 5 m/s raised to 20 m/s. The surface roughness of the workpiece reduction significantly (Figure 11(c)). Therefore, higher wheel speed can be selected to reduce grinding roughness. When the grinding wheel speed is too low, the cutting thickness of a single abrasive particle is large, which not only increases the surface roughness of the workpiece, but also increases the abrasive wear of the CBN grinding wheel.

The surface roughness of MoS_2-coated CBN wheel grinding is lower than that of common CBN wheel grinding titanium alloy. Because the lubricant exerts its effective lubricating effect in the grinding zone by forming a lubricating film on the grain surface. In the absence of solid lubricants, the surface of the grains is in direct contact with the wear debris, and the friction is relatively large. In the case of high temperature and high pressure, residues are formed, which stick to the surface of the workpiece or the grinding wheel, and even block and passivate the grinding wheel, therefore, a smaller surface roughness value cannot be obtained. Figure 12 shows the surface topography of the workpiece after grinding with two grinding wheels. It can be seen that there are a lot of built-up edge and grinding bond on the surface of titanium alloy with common CBN wheel. Due to the effective lubricating effect of MoS_2 lubricant, the ground surface morphology of MoS_2-coated CBN wheel has been greatly improved, and it is also more conducive to prolong the service life of grinding wheel.

4 Conclusions

(1) The MoS_2-coated CBN wheel enters the grinding state, and a layer of MoS_2 solid lubricating film exists between the workpiece surface and abrasive grains, the friction coefficient between the grain and the workpiece surface is diminished, consequently reducing the grinding force.

(2) Both the grinding force of MoS_2-coated CBN wheel and common CBN grinding wheel increase with the increase of grinding depth and feed speed, and decrease with the increase of wheel linear speed.

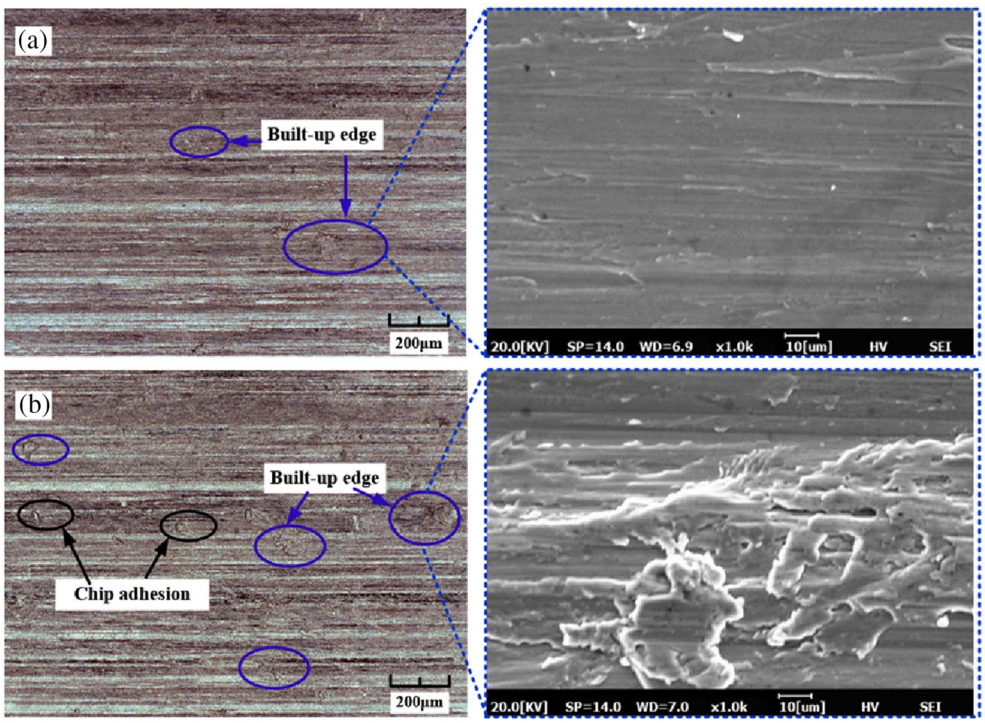

Figure 12 Comparison of ground surface morphology of two kinds of grinding wheels: (**a**) MoS_2-coated CBN wheel grinding and (**b**) common CBN wheel grinding

Among them, the grinding depth has the greatest impact on the grinding force, and the grinding force of MoS_2-coated CBN wheel is significantly lower than that of common CBN grinding wheel. Within the range of parameter selection, the normal grinding force F_n decreases by 42.5%, and the tangential grinding force F_t decreases by 28.1%.

(3) The grinding depth has the most significant effect on the grinding temperature. When the grinding depth increased from 5 μm to 20 μm, the grinding temperature of MoS_2-coated CBN wheel increased by 106.9%, while the grinding temperature of common CBN grinding wheel increased by 160.5%, and showed a sharp upward trend. There was no burn on the ground surface of the workpiece within the test parameters. MoS_2 lubricant provides a carrier for heat flow, reduces frictional heat energy and reduces grinding temperature.

(4) The wear of CBN grains of grinding wheel is analyzed through mathematical statistics method, and the wear of grains is quantified. The analysis shows that MoS_2 lubricant can essentially reduce the wear of CBN grains and prolong the service life of grinding wheel.

Acknowledgements
Not applicable.

Authors' Contributions
JZ, BZ and MH were in charge of the whole trial; JZ wrote the manuscript; WD, BW, JX and GL assisted with sampling and laboratory analyses. All authors read and approved the final manuscript.

Authors' Information
Junshuai Zhao born in 1992, is currently a PhD candidate at *Nanjing University of Aeronautics and Astronautics, China*. His main research interests include ultrasonic vibration assisted grinding and precision machining.
Biao Zhao born in 1991, is currently an assistant professor at *Nanjing University of Aeronautics and Astronautics, China*. His main research interests include the high-efficiency and high-quality grinding technology of aerospace high-strength, tough and difficult to machine materials and the preparation technology of high-performance superhard tools.
Wenfeng Ding born in 1978, is currently a professor at *Nanjing University of Aeronautics and Astronautics, China*. His main research interests include Grinding technology and equipment, superhard abrasive tool technology, machining process simulation and control technology.
Bangfu Wu born in 1991, is currently a PhD candidate at *Nanjing University of Aeronautics and Astronautics, China*. His main research interests include ultrasonic vibration assisted grinding and precision machining.
Ming Han born in 1999, is currently a master candidate at *Nanjing University of Aeronautics and Astronautics, China*. His main research interests include ultrasonic vibration assisted grinding.
Jiuhua Xu born in 1964, is currently a professor at *Nanjing University of Aeronautics and Astronautics, China*. His main research interests include high performance cutting / grinding technology, superhard abrasive tool technology and high-efficiency composite machining technology.
Guoliang Liu born in 1979, is currently an engineer at *AECC Zhongchuan Transmission Machinery Co., Ltd, China*. His main research interests include grinding of aerospace materials, design and manufacturing of gear transmission systems.

Funding
Supported by National Natural Science Foundation of China (Grant Nos. 92160301, 92060203, 52175415, 52205475), Science Center for Gas Turbine Project of China (Grant Nos. P2022-AB-IV-002-001, P2023-B-IV-003-001), Jiangsu Provincial Natural Science Foundation of China (Grant No. BK20210295), and Graduate Research and Innovation Projects in Jiangsu Province of China (Grant No. KYCX22_0339).

Declarations

Competing Interests
The authors declare no competing financial interests.

Received: 3 August 2022 Revised: 23 December 2022 Accepted: 24 August 2023
Published online: 20 September 2023

References

[1] X H Qian, X Y Duan, J Y Zou. Effects of different tool microstructures on the precision turning of titanium alloy TC21. *International Journal of Advanced Manufacturing Technology*, 2020, 106(6): 5519–5526.
[2] A Koreshkov, A Boitsov, M Siluyanova, et al. Electrospark alloying of titanium alloy aircraft engine parts. *Journal of Physics: Conference Series*, 2021, 1925(1): 012087 (11).
[3] S Yang, Y G Li, W H Li. Development of anti-fatigue surface modification technology of aeronautical titanium alloy. *Aeronautical Manufacturing Technology*, 2017, (13): 28-35.
[4] G G Zhang, Y L Sun, W L Fan, et al. Research progress and future development of surface integrity on machined surface of titanium alloys. *Aeronautical Manufacturing Technology*, 2022, 65(4): 36-55.
[5] Z Li, W F Ding, C Y Ma, et al. Grinding temperature and wheel wear of porous metal-bonded cubic boron nitride superabrasive wheels in high-efficiency deep grinding. *Proceedings of the Institution of Mechanical Engineers, Part B: Journal of Engineering Manufacture*, 2017, 231(11): 1961-1971.
[6] B Zhao, W F Ding, Y Zhou, et al. Effect of grain wear on material removal behaviour during grinding of Ti-6Al-4V titanium alloy with single aggregated CBN grain. *Ceramics International*, 2019, 45(12): 14842-14850.
[7] Q Miao, W F Ding, W J Kuang, et al. Comparison on grindability and surface integrity in creep feed grinding of GH4169, K403, DZ408 and DD6 nickel-based superalloys. *Journal of Manufacturing Processes*, 2020, 49: 175-186.
[8] X Zhao, Y D Gong, G Q Liang, et al. Face grinding surface quality of high-volume fraction SiC-(p)/Al composite materials. *Chinese Journal of Mechanical Engineering*, 2021, 34: 3.
[9] S Guo, W Du, Q H Jiang, et al. Surface integrity of ultrasonically-assisted milled Ti6Al4V alloy manufactured by selective laser melting. *Chinese Journal of Mechanical Engineering*, 2021, 34: 67.
[10] J D, C H Li, S Wang, et al. Investigation into distributing characteristic of suspend particulate in MQL grinding. *Manufacturing Technology and Machine Tool*, 2014, (2): 58-61.
[11] G F Zhang, X Deng, D Liu, et al. A nano-MQL grinding of single-crystal nickel-base superalloy using a textured grinding wheel. *The International Journal of Advanced Manufacturing Technology*, 2022, 121(3): 2787-2801.
[12] D Z Jia, C H Li, Y B Zhang, et al. Grinding performance and surface morphology evaluation of titanium alloy using electric traction bio micro lubricant. *Journal of Mechanical Engineering*, 2022, 58(5): 198-211. (in Chinese)
[13] B Zhao, W F Ding, G H Jiang, et al. Investigation on microstructure characteristics and tribological properties of self-lubricating metallic composites based on hexagonal boron nitride and molybdenum disulphide. *Journal of Tribology-Transaction of the ASME*, 2020, 143:021902.
[14] A Matthew, K Kyriaki, M Shreyes. An investigation of graphite nanoplatelets as lubricant in grinding. *International Journal of Machine Tools and Manufacture*, 2009, 49(12-13): 966-970.

[15] S Shaji, V Radhakrishnan. Analysis of process parameters in surface grinding with graphite as lubricant based on the Taguchi method. *Journal of Materials Processing Technology*, 2003, 141(1): 51-59.
[16] S Shaji, V Radhakrishnan. Application of solid lubricants in grinding: investigations on graphite sandwiched grinding wheels. *Machining Science and Technology*, 2003, 7(1): 137-155.
[17] B Rahmati, A Sarhan, M Sayuti. Morphology of surface generated by end milling AL6061-T6 using molybdenum disulfide (MoS2) nanolubrication in end milling machining. *Journal of Cleaner Production*, 2014, 66: 685-691.
[18] Y F Ding, W G Huo, X D Su, et al. A Grinding wheel of self-lubrication with solid powder lubricant and centrifugal impeller for green grinding process of TC4 alloy. *Key Engineering Materials*, 2017, 748: 269-274.
[19] S Mahathanabodee, T Palathai, S Raadnui, et al. Effects of hexagonal boron nitride and sintering temperature on mechanical and ribological properties of SS316L/h-BN composites. *Materials and Design*, 2013, 46: 588-597.
[20] K P Furlan, de Mello, J D B, et al. Self-lubricating composites containing MoS_2: A Review. *Tribology International*, 2018, 120: 280-298.
[21] X C Lu, S Z Wen, J B Luo. New progress in micro friction and wear research. *Journal of Tribology-Transactions of the ASME*, 1995, 15(2): 177-183.
[22] S S Akhtar. A critical review on self-lubricating ceramic-composite cutting tools. *Ceramics International*, 2021, 47(15): 20745-20767.
[23] W F Ding, Q Miao, B K Li, et al. Review on grinding technology of nickel-based superalloys used for aero-engine. *Journal of Mechanical Engineering*, 2019, 55(1): 189. (in Chinese)
[24] Y Wang, X Li, Y Wu, et al. The removal mechanism and force modelling of gallium oxide single crystal in single grit grinding and nanoscratching. *International Journal of Mechanical Sciences*, 2021, 204: 106562-106562.
[25] N Qian, Z C Zhao, Y C Fu, et al. Numerical analysis on temperature field of grinding Ti-6Al-4V titanium alloy by oscillating heat pipe grinding wheel. *Metals-Open Access Metallurgy Journal*, 2020, 10(5): 670.
[26] Z C Zhao, N Qian, W F Ding, et al. Profile grinding of DZ125 nickel-based superalloy: Grinding heat, temperature field, and surface quality. *Journal of Manufacturing Processes*, 2020, 57: 10-22.
[27] L Wang, L Y Wang, X J Tang, et al. Construction and analysis of grinding temperature model for gear processed by form grinding technology. *Journal of Mechanical Engineering*, 2022, 58(03): 295-304.
[28] A Naskar, A Choudhary, S Paul. Wear mechanism in high-speed superabrasive grinding of titanium alloy and its effect on surface integrity. *Wear*, 2020: 462-463.
[29] B K Li, Q Miao, M Li, et al. An investigation on machined surface quality and tool wear during creep feeding grinding of power metallurgy nickel-based superalloy FGH96 with alumina abrasive wheels. *Advances in Manufacturing*, 2020, 8 (2): 160-176.
[30] G J Xiao, Y D Zhang, Y Huang, et al. Grinding mechanism of titanium alloy: research status and prospect. *Journal of Advanced Manufacturing Science and Technology*, 2021, 2020001.
[31] R Reizer. Simulation of 3D Gaussian surface topography. *Wear*, 2011, 271(3): 539-543.
[32] X M Mu, Q C Sun, J W Xu, et al. Feasibility analysis of the replacement of the actual machining surface by a 3D numerical simulation rough surface. *International Journal of Mechanical Sciences*, 2019, 150: 135-144.
[33] B F Wu, B Zhao, W F Ding, et al. Investigation of the wear characteristics of microcrystal alumina abrasive wheels during the ultrasonic vibration-assisted grinding of PTMCs. *Wear*, 2021, 477(427): 203844.